

# Improved maximum power point tracking algorithms by using numerical analysis techniques for photovoltaic systems

Lyu Guanghua<sup>a</sup>, Farah Andleeb Siddiqui<sup>b,\*\*</sup>, Muhammad Mohsin Aman<sup>b</sup>,  
Syed Hadi Hussain Shah<sup>a,\*</sup>, Aqsa Ali<sup>c</sup>, Arsalan Muhammad Soomar<sup>d</sup>, Shoaib Shaikh<sup>e</sup>

<sup>a</sup> Power China Huadong Engineering Co., Ltd., Hangzhou, China

<sup>b</sup> Electrical Engineering Department, NED University of Engineering and Technology, Karachi, Pakistan

<sup>c</sup> Mohammad Ali Jinnah University, Karachi, Pakistan

<sup>d</sup> Faculty of Electrical and Control Engineering, Gdańsk University of Technology, Gdańsk, Poland

<sup>e</sup> Department of Electrical Engineering, Mehran University of Engineering and Technology, Jamshoro, Pakistan

## ARTICLE INFO

### Keywords:

Solar  
Renewable energy  
MPPT  
Numerical analysis technique  
Algorithm

## ABSTRACT

Solar photovoltaic (PV) panels generate optimal electricity when operating at the maximum power point (MPP). This study introduces a novel MPP tracking algorithm that leverages the numerical prowess of the predictor-corrector method, tailored to accommodate voltage and current fluctuations in PV panels resulting from variable environmental factors like solar irradiation and temperature. This paper delves into the intricate dynamics of solar panels, presenting a comprehensive mathematical model capturing the interdependencies between current, voltage, power, solar irradiation, and temperature. Existing numerical MPPT techniques are explored to provide their advantages and disadvantages. The proposed algorithm, formulated in MATLAB, encapsulates essential solar panel variables and undergoes rigorous dynamic testing in the Simulink® environment under diverse solar irradiation and temperature scenarios. These results are visually represented through graphs and tabulations. A subsequent section offers a simulation-driven comparative review of the proposed algorithm against established methodologies. The article culminates with conclusions drawn from the empirical findings and outlines promising avenues for future research.

## 1. Introduction

Energy is one of the major factors that improve living quality. Still, constraints like global warming, climate changes, world energy demand, and the limitation of fossil fuel reserves compel the masses to search for new energy resources. Globally, there has been a shift from fossil fuel to renewable power generation. Photovoltaic power generation plays a significant role because they do not emit greenhouse gases and is environmentally friendly. It could be installed feasibly where it is difficult to supply power through electricity networks. However, it requires significant focus where the maximum power point is concerned. The voltage-current relation of the PV array is non-linear, as shown in Fig. 1, with a unique point at which the power produced is maximum. The PV system should continuously operate near or at this point. In recent years, due to the energy crisis and environmental concerns, countries around the world have been focusing on green technology, where solar energy

has grown as one of the most potent forms of renewable energy [2,3].

The problem associated with this point is that it varies with environmental conditions like Temperature and solar irradiance. Thus, the MPPT algorithm was needed [4] [5]. Many techniques have been developed for this purpose, each with pros and cons, and many improved, efficient, and practical algorithms are still in their research phase. The efficiency of solar panels depends on the MPPT algorithm, so modified algorithms with better functionality are always in demand. Numerical techniques like Newton-Raphson, secant method, bisection methods, etc., provide a balance between efficiency and complexity. In this paper, the numerical scheme of the predictor-corrector method concerning solar PV panels has been implemented. Due to the high initial cost, it is required to operate a solar photovoltaic (SPV) system at its MPP for a given solar insolation level [6].

\* Corresponding author.

\*\* Corresponding author.

E-mail addresses: [siddiquifarrah19@gmail.com](mailto:siddiquifarrah19@gmail.com) (F.A. Siddiqui), [Hadihussain010@gmail.com](mailto:Hadihussain010@gmail.com), [hadi.shah@jinnah.edu](mailto:hadi.shah@jinnah.edu) (S.H. Hussain Shah).

<https://doi.org/10.1016/j.rineng.2023.101740>

Received 29 October 2023; Received in revised form 27 December 2023; Accepted 30 December 2023

Available online 8 January 2024

2590-1230/© 2024 The Author(s). Published by Elsevier B.V. This is an open access article under the CC BY license (<http://creativecommons.org/licenses/by/4.0/>).

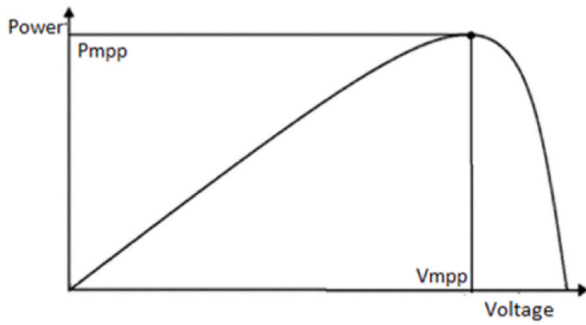


Fig. 1. Power Vs. Voltage curve of solar panel [1].

2. I-V & P-V characteristics of solar panels

The solar cell may be modeled majorly in three different ways [7]; Chawdry, 2007 [8]; however, the diode model of Solar Panel, with its simplicity and ease of adjusting the parameters, makes it feasible to be used at large [9]. Fig. 2 shows the single diode equivalent model with ideal and practical modeling of PV cells [11,12].

Applying KCL in Fig. 2 yields as shown in equations (1) and (2) [10].:

$$I = I_{ph} - I_D - I_{sh} \tag{1}$$

$$I = I_{ph} - I_{sat} \left[ \left( \exp \exp \frac{V + IR_s}{nN_s V_{th}} \right) - 1 \right] - \left( \frac{V + IR_s}{R_{sh}} \right) \tag{2}$$

Where  $N_s = a$  number of series connected solar cells. Series connection increases voltage, so the factor is multiplied by voltage. If the cells are connected in parallel, then:

$$I_{ph} = N_p I_{ph}; I_{sat} = N_p I_{sat}; \tag{3}$$

$N_p =$  parallel connected mod ules

Parallel connection increases the current, so the current multiplies the factor.

$R_s =$  Equivalent series resistance of the array

$R_{sh} =$  equivalent parallel resistance of the array.

The solar panel gives a DC output, so the resulting power from a solar panel can be found using the following equation:

$$P_{dc} = V * I \tag{4}$$

Multiplying eq. (2) with the PV terminal voltage, we get:

$$P = V \left\{ I_{ph} - I_{sat} \left[ \left( \exp \exp \frac{V + IR_s}{nN_s V_{th}} \right) - 1 \right] - \left( \frac{V + IR_s}{R_{sh}} \right) \right\}$$

If we plot Eq. (1) (ignoring parallel resistance drop  $I_{sh}$ ), the resulting plot is the I-V characteristic of solar panels, as shown in Fig. 3.

The P-V characteristic of solar panels is shown in Fig. 4 as a result of plotting eq. IV concerning different solar voltages.

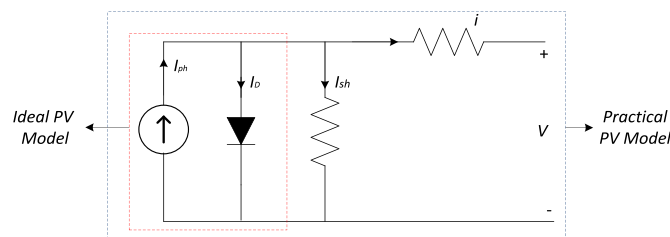


Fig. 2. Diode model for PV cell [10].

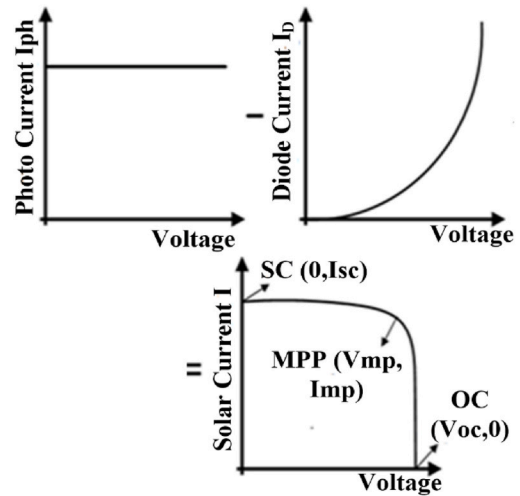


Fig. 3. Current Vs. Voltage of PV panel [13].

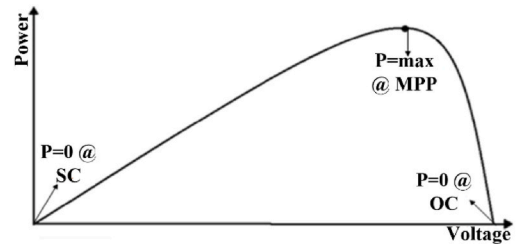


Fig. 4. Power of Solar PV Panel at three conditions [13].

3. Maximum power point and its variation with temperature (t) and solar irradiation (G)

A solar panel's I-V and P-V characteristics reveal a non-linear relationship between the three quantities. Which results in three essential points:

1. **Open circuit condition ( $V_{oc}, 0$ ):** An operating point where the panel's output current is zero and the terminal voltage is maximum.
2. **Short circuit condition ( $0, I_{sc}$ ):** An operating point where the panel's output voltage is zero, and the solar panel gives maximum current output.
3. **Maximum Power Point ( $V_{MP}, I_{MP}$ ):** An operating point where the panel's output voltage and output current are such that their product (power) is maximum.

If the above two points are replaced in equation (4), the resulting solar power would be zero.

Since the efficiency of the complete solar generation system depends upon its power output, tracking the maximum power point is essential. Chasing this entire power point becomes crucial because the PV panel's voltage and current vary with the environmental effect. Temperature and solar irradiance are the two factors that should be considered. This variation is governed by the following pair of eqs. (5) and (6) [14].:

$$V_{oc}(G, T) = V_{oc}^* + \frac{N_s K T n}{q} \ln \ln \left( \frac{G}{G^*} \right) + \mu_{oc}(T - T^*) \tag{5}$$

$$I_{sc}(G, T) = [I_{sc}^* + \mu_{sc}(T - T^*)] \frac{G}{G^*} \tag{6}$$

As a result, the MPP varies and has to be tracked around

continuously. The variation in the short circuit current or photo-generated current and open circuit voltage and hence power concerning change in irradiation is shown in Figs. 5 and 6. The effect of changing atmospheric condition was simulated on SunPower SPR-305E-WHT-D on MATLAB Simulink.

The photocurrent is directly proportional to the irradiance level, whereas the effect of solar irradiance on voltage is logarithmic and is usually ignored. The result of Temperature on the variation of voltage, current, power, and MPP is illustrated in Figs. 7 and 8.

The Temperature has little effect on the short circuit current level because the temperature change is multiplied by the temperature coefficient for short circuit current, and its value for silicon is negligible. The open circuit voltage has a negative temperature coefficient, which indicates that as the Temperature of the cell increases, its open circuit voltage decreases [14].

4. Numerical analysis techniques for MPPT

Several numerical method techniques provide a much better option for tracking maximum power points. All the numerical method techniques available offer fast convergence and speedy response. They can have flexible step sizes and no oscillations once the system reaches the maximum power point. The NMs are therefore used to find the best-fit value for the equation through several subsequent iterations [15]; Metwally, Hassan & Mourad, 2016).

The root-finding methods can be better understood from Fig. 9. According to Ref. [16], they are divided into two categories:

1. Open Bracket methods: These are not bound by any interval. Generally, it converges rapidly, but the convergence and stability of the system are not guaranteed. If the initial approximation is not chosen correctly, then they might diverge or take a longer time/step to converge.
2. Close bracket methods: They are bounded by a closed interval. It is slower to converge, but the convergence is guaranteed.

4.1. Newton-Raphson method

NR method has been employed by many researchers [17–23]; Rektenwald, 2015 [24–26]; either for tracking the maximum power point or for finding the parameters of the solar PV panel. This method uses the function as well as the derivative of the function. Suppose the derivative is not known, and this method is not applicable. The following equation is used:

$$Y_{n+1} = Y_n - \frac{f(Y_n)}{f'(Y_n)} \tag{7}$$

So, only an initial guess is to be chosen. For maximum power point, cap Y sub n can be the voltage value, and f open paren cap Y sub n, close paren equals d cap P over d cap V. Accordingly, the function's derivative will be the curve's second derivative. Hence, the drawback of this method is that more computations are required, and if the tangent becomes parallel to the x-axis at some point, this method will not work.

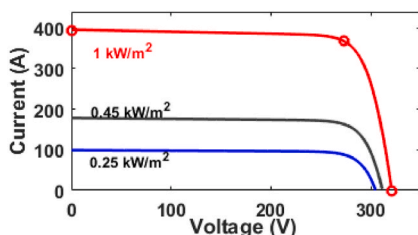


Fig. 5. Variation of voltage and current with solar irradiation [14].

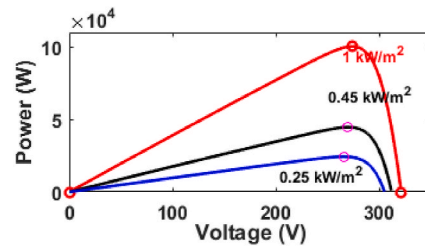


Fig. 6. Variation of power with change in solar irradiation [14].

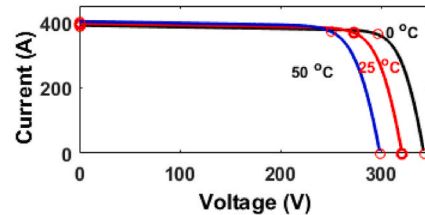


Fig. 7. Change in current and voltage with temperature [14].

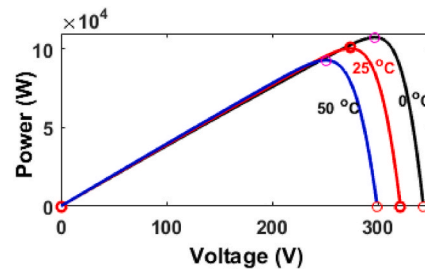


Fig. 8. Change in current and voltage with temperature [14].

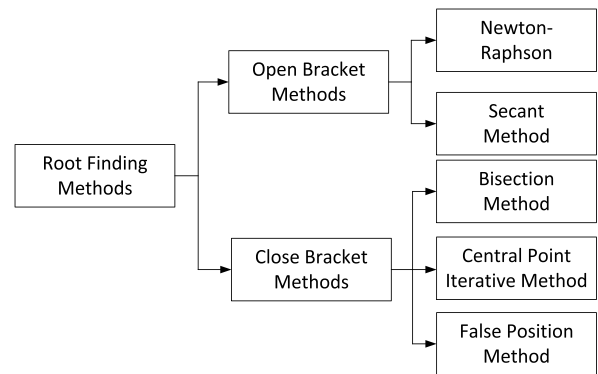


Fig. 9. Classification of root-finding method.

Also, selecting a topic far away from the root can mislead into divergence. Another drawback of this method, as stated in Ref. [27] is that a very narrow interval of initial guess will converge the solution to MPPT.

4.2. secant method

NR, being efficient, sometimes becomes computationally expensive because of the required derivative. The second method, as used in Ref. [28], is another option for tracking the maximum power point. In this method, the derivative is estimated using two initial guesses close to one another. The following equation is used:

$$Y_n = Y_{n-1} * f(Y_{n-1}) \left( \frac{(Y_{n-1}) - (Y_{n-2})}{f(Y_{n-1}) - f(Y_{n-2})} \right) \quad (8)$$

Here again  $Y_n$  could be the voltage and  $f(Y_{n-1}) = \frac{dP}{dV}$  for tracking the solar maximum power point. The drawback of this method is that stability and convergence cannot be guaranteed if the second guess is too far or too close to the first guess. Also, like NR, it is susceptible to slope values close to zero.

#### 4.3. Bisection method

The bisection method [29]; Soediby, 2013 [30]; is a close bracketed technique. The interval is always chosen in such a way that  $f(Y_L)f(Y_U) < 0$ . For this method the convergence is guaranteed but it tends to respond slower as compared to open bracketed method. The bisection method does not account for the value of the function; instead, it uses the sign of the function for the convergence, which makes it slower. This method is also known as interval halving since it divides the interval into two equal sub-intervals. It utilizes the following equation [31]:

$$Y_m = \frac{Y_U + Y_L}{2} \quad (9)$$

Where  $Y_U$  = upper limit bound

$Y_L$  = lower limit bound

$Y_m$  = mid-point for each iteration.

For maximum power point, the interval is chosen as  $[0, Voc]$  and the  $f(V) = \frac{dP}{dV}$ . The system always converges in the direction of  $f(0)f(Voc) < 0$ . The following steps are used:

1. Select an appropriate interval such that  $Y_L \neq Y_U$  and  $f(Y_L)f(Y_U) < 0$ .
2. Find the mid-point using equation (xi).
3. Find the value of the function at the mid-point i.e.  $f(Y_m)$ .
4. If  $f(Y_L)f(Y_m) < 0$ , then replace  $Y_U = Y_m$ , otherwise, replace  $Y_L = Y_m$ .
5. Repeat from step # 2, until the system reaches a desired accuracy level.

#### 4.4. Central point iterative method

Like any other numerical technique, the variable and function are the same for MPP tracking. In this method, as used in Refs. [32–34]. [35] the control variable, which in our case is the Voltage or Current of the PV panel, is divided into four non-overlapping intervals giving three points. The desired output, which in our case is the power of the PV panel, is calculated and compared. After comparison, two out of four intervals with a higher probability of having MPP are selected, and the process continues. Since the limits bound the intervals, it comes under the head of the close bracketed technique.

#### 4.5. Regula falsi method

This method is the same as the second method but with the difference that it has close intervals that contain the equation's root. This method also resembles the bisection method, but it is far more efficient compared to that because it calculates the weighted average according to the following equation (10) (Shun and Kwasinski, 2011):

$$C_{n+1} = \frac{Y_n - f(Y_n) - Y_{n-1}f(Y_{n-1})}{f(Y_n) - f(Y_{n-1})} \quad (10)$$

It can be considered a hybrid technique of the secant and bisection methods. It feels the value of the function and not just the sign. The RFM always leaves one endpoint of the interval fixed, which generates an opportunity for improvement (Shun and Kwasinski, 2011 [36]; Young & Mohlenk, 2018; Yang et al., 2015) [37,38].

## 5. Predictor-corrector-based MPPT proposed algorithm

Predictor-corrector scheme comes under the umbrella of numerical analysis techniques used to solve ordinary differential equations. It is used to find an unknown function that satisfies a given differential equation. Predictor-corrector is a multistep procedure. It is a combination of an explicit and implicit method. A precise way is the one in which the values at previous points are given, and the current threshold has to be calculated. The generalized equation (11) for the explicit method can be provided by (Yang et al., 2015):

$$X_{(n+1)} = \sum_{i=1}^n X_i + h \sum_{i=1}^n f(X_i) \quad (11)$$

An implicit method finds the value at the current point using the previous and the current value. The current threshold value is either approximated using some explicit method or an approximation is needed. It is usually more accurate than the straightforward method but more time-consuming. The generalized equation for the implicit process can be given by:

$$X_{(n+1)} = \sum_{i=1}^{n+1} X_i + h \sum_{i=1}^{n+1} f(X_i) \quad (12)$$

In the predictor-corrector method, an explicit method calculates the initial value at a particular point instead of assuming an initial guess. Then, that value is used in an implicit approach to refine that value further with greater accuracy. The simplest form of the predictor-corrector process is Euler's Trapezoidal rule. However, this method is unnecessary, and any explicit-implicit technique can be implemented. The following equations give the two steps of predictor and corrector:

Consider a differential equation:

$$y' = f(t, y) \quad y(t_0) = y_0$$

Where  $y'$  = differential equation

$y_0$  = initial value of the variable on which the differential equation depends.

- Predictor step:

$$y_{i+1}^p = y_i + hf(t_i, y_i) \quad i \in R; \geq 0 \quad (13)$$

Where  $h$  = step – size

- Corrector-step:

$$y_{i+1}^c = y_i + \frac{1}{2} h \{ f(t_i, y_i) + f(t_{i+1}, y_{i+1}^p) \} \quad (14)$$

One iteration is completed after this step. So far, the step size has not been discussed, but it is evident that the accuracy of the calculation is strongly dependent on the value chosen for the step size. If  $h$  is chosen too large, the calculated solution will deviate from the actual value of the differential equation. If picked too small, the computation will become unnecessarily time-consuming, increasing the roundoff error.

#### 5.1. Linking MPPT and predictor-corrector technique

The output power of the solar panel is given in equation (15). For the predictor-corrector method, this equation is differentiated concerning the solar PV voltage and results in:

$$\frac{dP}{dV} = I_{ph} + I_{sat} \left[ 1 - \exp \left( \frac{V}{nN_s V_{th}} \right) \left\{ \frac{V}{nN_s V_{th}} + 1 \right\} \right] - \left( \frac{2V'}{R_{sh}} \right) = f(V_i) \quad (15)$$

Since the value of series resistance is minimal, so it does not create a significant voltage drop across it. Therefore, the product of IRs could be easily neglected without causing any computational error.

Equations (16)–(18) links the numerical method with solar PV panels.

$$V_{i+1}^p = V_i + hf(V_i) \quad i \in R; i \geq 0 \quad (16)$$

$$V_{i+1}^c = V_i + \frac{1}{2}h\{f(V_i) + f(V_{i+1}^p)\} \quad (17)$$

$$f(V_i) = \frac{dP_i}{dV_i} \quad (18)$$

The initial value of solar voltage  $V_0$  is taken in between 75 % and 80 % of the open circuit voltage at given solar irradiance and temperature condition. The initial voltage can start from 1V, but converging would take too long. It has been approximated that the maximum power point voltage is in between 70 % and 90 % of the open circuit voltage according to the fractional open circuit voltage scheme. This information can be utilized for the initialization of the predictor-corrector method.

## 5.2. Flowchart of Proposed Algorithm

Fig. 10 shows the flow of the proposed algorithm as it is applied to the solar PV panel to locate the voltage value at the maximum power point. The abbreviations used in the flow chart are given below:

**Voc** = open circuit voltage on Standard testing condition.

**Isc** = short circuit current at standard testing condition.

**Ns** = number of series connected cells

**$\mu_{oc}$**  = temperature coefficient of open circuit voltage

**$\mu_{sc}$**  = temperature coefficient of short circuit current.

**Rsh** = shunt resistance.

**n** = diode ideality factor.

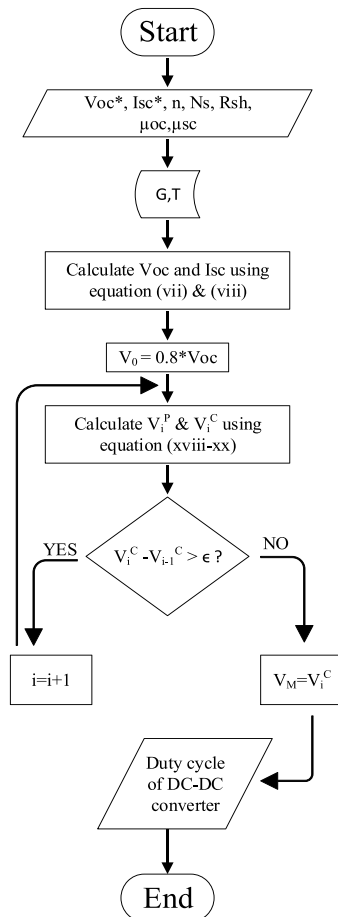


Fig. 10. Flowchart of proposed algorithm.

**G** = solar irradiance in  $W/m^2$ .

**T** = Temperature in  $^{\circ}C$ .

**i** = index number.

**$V_{i+1}^p$**  = predictor value of solar panel voltage.

**$V_{i+1}^c$**  = corrected value of the solar panel voltage.

The predictor-corrector method is PV panel dependent and uses specific parameters of the panel to calculate the function value. Some of these parameters are available on the datasheet, and some can be calculated using Newton-Raphson.

## 6. Implementation of the proposed algorithm

This section deals with implementing the proposed Algorithm in the MATLAB Simulink® model. It comprises a 100 kW PV array connected to the 25 KV grid through a DC-DC boost converter and a three-phase, three-level Voltage Source Converter (VSC). The Maximum Power-Point tracking controller has been interfaced between the output of the PV panel and the DC-DC converter. This block implements the Algorithm that has been proposed using the predictor-corrector method. The model developed is average because the boost and VSC converters are represented by equivalent voltage sources generating the AC voltage averaged over one cycle of the switching frequency. In this model, the harmonics of the system are not represented. However, the resulting power system and control system interaction dynamic are preserved. The average model is simulated much more efficiently compared to the detailed model. The electrical parameters are discretized at  $50\mu s$ . For the control system, the sample time is  $100\mu s$ . The MATLAB®/Simulink® model for the implementation with all components is shown in Fig. 11.

### 6.1. Solar PV panel

A commercial solar panel Sunpower-SPR305E-WHT-D was selected with five series connected and 66 parallel connected strings. The module's output power is 305.226W, which, when multiplied by several series and parallel modules, gives 100.724 kW ( $66 * 5 * 305.226$ ).

Table 1 gives the solar panel's module and model parameters under consideration. The manufacturer specifies the module parameters on the datasheet, but the model parameters are to be determined using some iterative technique. The value of  $R_s$  may vary depending on the insolation and temperature. For the given conditions in Table 2, The value of  $R_s$  is 677 m $\Omega$ , 742 m $\Omega$  and 924 m $\Omega$  (at 1100  $W/m^2$ , 1000  $W/m^2$  and 800  $W/m^2$ ). Moreover, for the given conditions in Table 3, the value of  $R_s$  is 677 m $\Omega$ , 717 m $\Omega$  and 742 m $\Omega$  (at 45  $^{\circ}C$ , 35 $^{\circ}$  and 25  $^{\circ}C$ ). Therefore, the value of  $R_s$  is very small and may be negligible.

For ease, the following consideration was made:

$$I_{ph} \approx I_{sc}$$

$$R_s \approx 0$$

### 6.2. Application of proposed algorithm

The proposed algorithm was incorporated into the simulation model and the defined PV panel selection. The system was tested individually for different irradiation and temperatures, and the results were compared with the theoretical results. The percentage error and the efficiency for each case were calculated.

### 6.3. Change in Solar Irradiation

Table 2 shows the actual and tested results of power and voltage. The efficiency and the percentage error were calculated using the following equation:

$$\eta = \frac{P_{Tested\ Value}}{P_{Actual\ Value}} * 100 \quad (19)$$



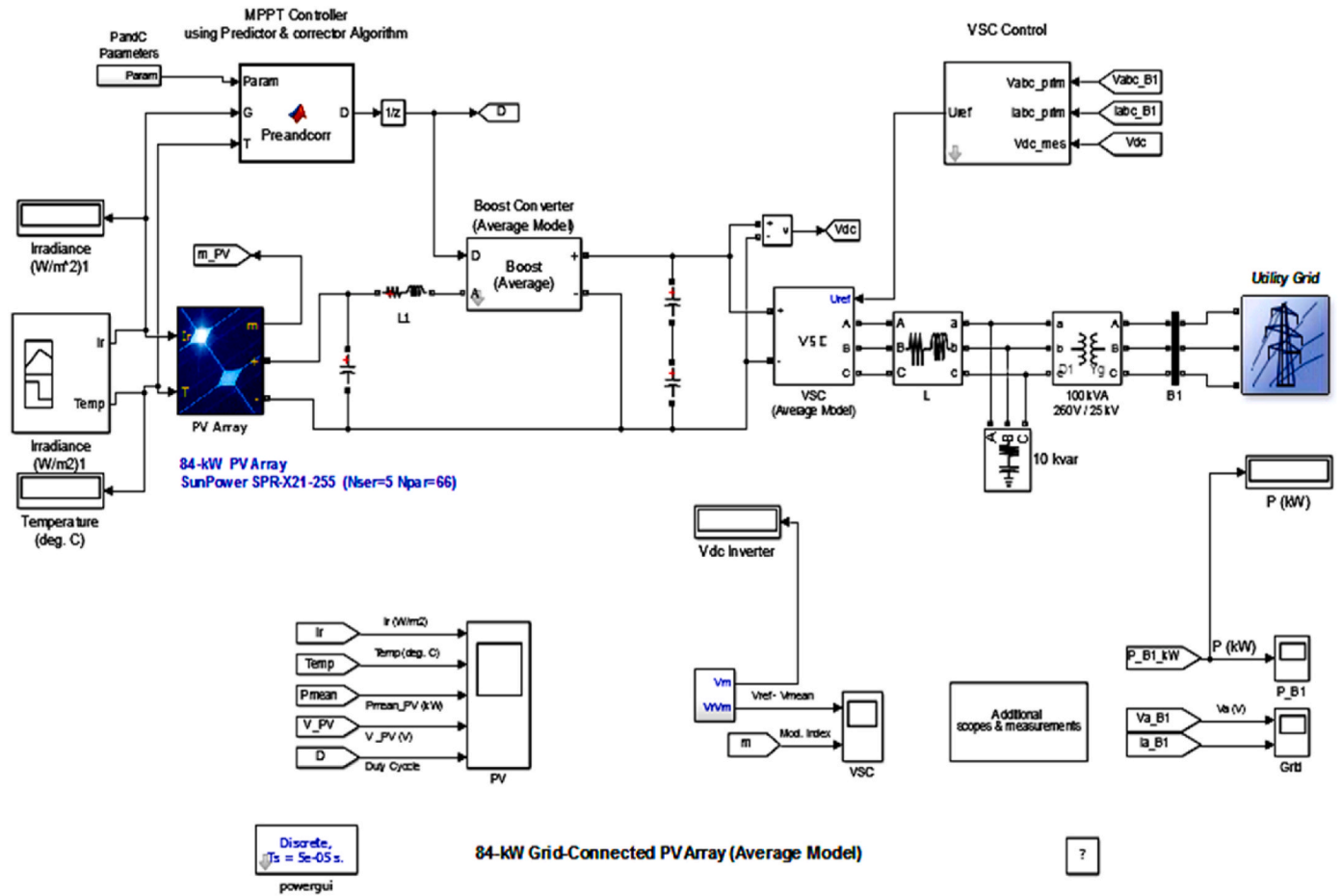


Fig. 11. Experimental Setup for testing of the Algorithm.

Table 1 Specifications of solar panel.

| Parameters        | Specification and symbol | Value & Units              |
|-------------------|--------------------------|----------------------------|
| Module parameters | $P_m$                    | 305.226 W                  |
|                   | $V_{oc}$                 | 64.2 V                     |
|                   | $I_{sc}$                 | 5.96 A                     |
|                   | $V_m$                    | 54.7 V                     |
|                   | $I_m$                    | 5.58 A                     |
|                   | $N_{cell}$               | 96                         |
|                   | $M_{oc}$                 | -0.27269 %/°C              |
| Cell parameters   | $M_{sc}$                 | 0.061745 %/°C              |
|                   | $R_{sh}$                 | 269.5934 Ω                 |
|                   | $N$                      | 0.94504                    |
|                   | $I_{sat}$                | $6.3014 \times 10^{-12}$ A |

$$\% \text{ Error} = \frac{\text{actual} - \text{tested}}{\text{actual}} * 100 \tag{20}$$

The Temperature for each of the following cases is taken as 25 °C. From Tables 2 and it can be seen that the voltage change is not very significant with the change in irradiation. However, power is noticeable

Table 3 Results of the proposed Algorithm at different temperatures.

| Temp °C | Power in KW |          |       |         | Voltage in V |          |         |
|---------|-------------|----------|-------|---------|--------------|----------|---------|
|         | Actual P    | Tested P | η%    | Error % | Actual V     | Tested V | Error % |
| 10      | 104.7       | 103.6    | 98.94 | 1.06    | 287.3        | 278      | 3.23    |
| 15      | 103.3       | 102.9    | 99.61 | 0.39    | 282.8        | 277.9    | 1.73    |
| 25      | 100.7       | 100.4    | 99.7  | 0.3     | 273.5        | 274.41   | 0.33    |
| 35      | 97.43       | 97.41    | 99.97 | 0.03    | 264.4        | 265.1    | 0.264   |
| 45      | 94.43       | 93.93    | 99.47 | 0.53    | 254.7        | 257.2    | 0.98    |

Table 2 Results at different solar irradiation.

| Solar Irradiation W/m² | Power in KW |          |       |        | Voltage in V |          |        |
|------------------------|-------------|----------|-------|--------|--------------|----------|--------|
|                        | Actual P    | Tested P | η%    | Error% | Actual V     | Tested V | Error% |
| 1100                   | 110.4       | 110.3    | 99.9  | 0.1    | 273.5        | 270.3    | 1.17   |
| 1000                   | 100.7       | 100.4    | 99.7  | 0.3    | 273.5        | 274.4    | 0.33   |
| 800                    | 80.17       | 80.11    | 99.9  | 0.1    | 272.3        | 275      | 0.99   |
| 600                    | 59.87       | 59.87    | 100   | 0      | 271.8        | 271.6    | 0.07   |
| 400                    | 39.55       | 39.52    | 99.9  | 0.1    | 268.7        | 266.8    | 0.707  |
| 250                    | 24.37       | 24.32    | 99.8  | 0.2    | 265.1        | 261.3    | 1.433  |
| 150                    | 14.36       | 14.31    | 99.65 | 0.35   | 260.4        | 258      | 0.923  |

because the  $I_{sc}$  is directly proportional to the irradiation level, and power, being the product of both voltage and current, varies substantially. The Algorithm's efficiency can be safely stated as 99 % on average with changing solar irradiation with best results from  $800W/m^2$  to  $400W/m^2$ .

6.4. Change in temperature

Like in the above section, the Temperature remained fixed at  $25\text{ }^\circ\text{C}$  and the irradiation was varied. The second condition was to keep the irradiation set at  $1000\text{ W/m}^2$ , individually change the Temperature, and record the power and voltage output. The observations for this case are presented in Table 3.

6.5. Dynamic testing of algorithm

The system was dynamically tested by changing the combination of irradiation and Temperature. The conditions according to simulation time are presented in Table 4. The panel's power, voltage, and current output are shown in Fig. 12.

It can be seen from Fig. 12 that the variation in the output voltage is not much. As the temperature increases from 2 to 4s of simulation time and the irradiance increases, the output voltage decreases due to the negative temperature coefficient. The irradiation has minimal effect on voltage change.

The power change occurs due to a significant change in current corresponding to the value of output PV voltage. The current and power follow the same curve as in Fig. 12 with the changing Temperature and irradiation. The current increases with the increase in irradiation as well as Temperature. Dynamic testing is essential to determine how the Algorithm responds to changing Temperature and irradiance. The less time it takes to adjust, the more efficient the Algorithm is.

7. Simulation-based comparison

A simulated comparison was initially investigated to verify the proposed Algorithm and evaluate it with the existing Algorithm regarding speed and accuracy. Arguably, the most common method, P&O, and one numerical method, the Bisection method, were considered. Perturb and observation, though simple implementation, resulted in power loss due to oscillations around MPP. The bisection method is one of the efficient methods that guarantees the convergence of the MPP, but its speed is slower than that of open bracket methods. The three algorithms were compared concerning MPPT tracking accuracy, speed of achieving the MPP, and evenness at steady state point.

As discussed in the implementation section, the three algorithms were simulated using the Simulink® model. The experiment was done on a commercial solar panel with specifications in Table 1, available in the NREL database of Simulink PV block under three different solar irradiation conditions and Temperatures. The results for each case are discussed in tabular and graphical form in this section. The actual power, voltage, and current values at different conditions for the system having this panel are specified in Table 5.

7.1. Study case # 1

The first condition is when the irradiance is  $1000W/m^2$ , and the

Table 4  
Dynamic result of the proposed Algorithm.

| Simulation Time | Solar Irradiation | Tempe            | Power O/p |
|-----------------|-------------------|------------------|-----------|
| s               | $W/m^2$           | $^\circ\text{C}$ | KW        |
| 0-2             | 800               | 25               | 79.89     |
| 2-4             | 1000              | 35               | 97.24     |
| 4-6             | 400               | 25               | 39.52     |

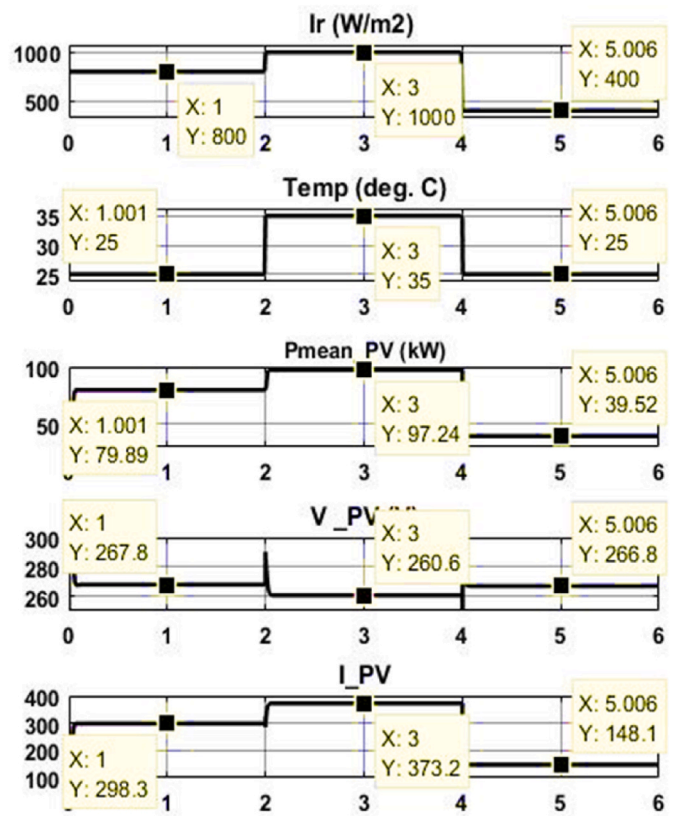


Fig. 12. Power, Voltage, and Current output of solar panel at dynamic testing.

Table 5  
Actual values of solar panels at different conditions.

| Condition                | Actual $P_m$ | Actual $V_m$ | Actual $I_m$ |
|--------------------------|--------------|--------------|--------------|
| $W/m^2$ $^\circ\text{C}$ | KW           | V            | A            |
| 1000    25               | 100.7        | 273.5        | 368.3        |
| 250    25                | 24.37        | 265.1        | 91.93        |
| 1000    40               | 95.93        | 259.9        | 369.1        |

Temperature is  $25\text{ }^\circ\text{C}$ . The result of the comparison is shown in Fig. 13 and Table 6.

The table shows that the response time for the Proposed Algorithm is the least, and the tracked value for all three algorithms is almost the same with slight differences. At the steady state, there are no oscillations for the proposed Algorithm.

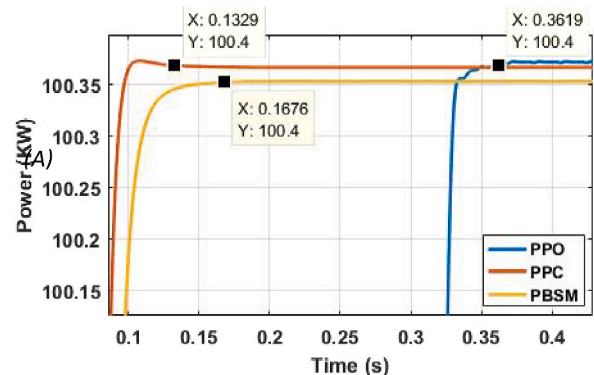


Fig. 13. Power of three algorithms for Case-1.

**Table 6**  
Summary of result for Case-1.

| Algorithm           | Power (KW) | Time (ms) |
|---------------------|------------|-----------|
| Predictor-corrector | 100.373    | 132.9     |
| Bisection Method    | 100.357    | 167.6     |
| Perturb and Observe | 100.379    | 361.9     |

7.2. Study case # 2

The second condition is when the irradiance is 250 W/m<sup>2</sup>, and the Temperature is 25 °C. The comparison result is shown in Fig. 14 and Table 7.

7.3. Study case # 3

The third condition is when the irradiance is 1000 W/m<sup>2</sup>, and the Temperature is 40 °C. The comparison result is shown in Fig. 15 and Table 8.

7.4. Result discussion

From the three experimental results, the following deductions can be made:

- The proposed Algorithm using a predictor-corrector scheme efficiently tracks the panel’s maximum power point for all types of irradiances and Temperatures.
- For each case, it can be observed that the convergence time for the proposed Algorithm was minimal compared to the other two methods.
- The numerical method techniques of predictor-corrector and bisection method reach the desired point in less time compared to analytical techniques such as perturb and observe.
- It can also be observed in the detailed signal view of power output that perturbs and observes the system oscillates around the maximum power point. Some of these variations are large; in others, they are not much but cause a loss of power. The system reaches the steady state smoothly for the other two methods, and no oscillations are observed.
- Among the three methods compared, the predictor-corrector algorithm approaches the correct maximum power point with a very slight deviation from the actual value in a minimum period and without having oscillations.

The comparison between the above three techniques has been summarized in Table 9.

8. Conclusion

In this study, a Maximum Power Point Tracking (MPPT) algorithm

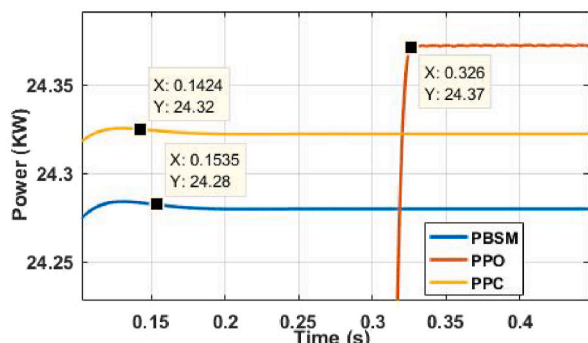


Fig. 14. Power of three algorithms for Case-2.

**Table 7**  
Summary of results for Case 2.

| Algorithm           | Power (KW) | Time (ms) |
|---------------------|------------|-----------|
| Predictor-corrector | 24.321     | 142.4     |
| Bisection Method    | 24.281     | 153.5     |
| Perturb and observe | 24.372     | 327.187   |

The table shows that the response time for the Proposed Algorithm is the least, and the tracked value for all three algorithms is almost the same with slight differences. The P&O oscillates when it reaches the Maximum power point.

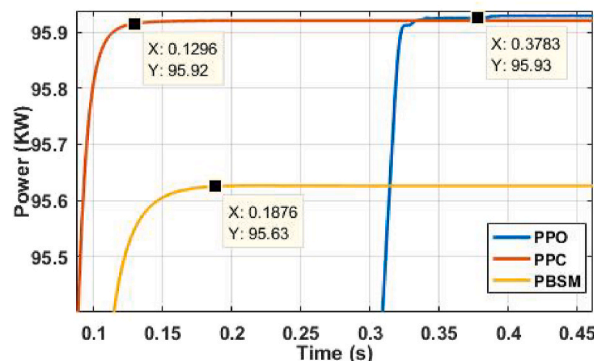


Fig. 15. Power of three algorithms for Case-3.

**Table 8**  
Summary of results for case 3.

| Algorithm           | Power (KW) | Time (ms) |
|---------------------|------------|-----------|
| Predictor-corrector | 95.918     | 129.6     |
| Bisection Method    | 95.635     | 187.6     |
| Perturb and observe | 95.929     | 378.3     |

The table shows that the response time for the Proposed Algorithm is the least, and the tracked value for all three algorithms is almost the same with slight differences. The P&O oscillates when it reaches the Maximum power point.

was developed utilizing a numerical analysis technique and subsequently validated using three distinct solar panels. Testing parameters included variations in irradiation at a consistent temperature of 25 °C, temperature alterations at a fixed irradiation of 1000W/m<sup>2</sup>, and a dynamic assessment wherein both variables were modified concurrently. Two benchmark methods were employed to provide a comparative analysis: the analytical “Perturb and Observe” and the numerical “Bisection Method.” Despite varying PV panels, a consistent simulation model was applied throughout the study, with the panels sourced from NREL’s commercial database. Comparative results demonstrated that numerical techniques outperform their analytical counterparts in convergence speed without oscillation once the desired point is achieved. Notably, the Predictor-corrector method displayed faster convergence than the Perturb and Observed and Bisection method, providing 2.3 times faster and 1.44 times faster than the Bisection method. Impressively, the proposed algorithm showcased an efficiency nearing 99 %. It is pivotal to note that these conclusions are rooted in simulation outcomes, devoid of experimental verification. However, the proposed research could be further enhanced by testing various dynamic conditions such as floating cloud conditions, rainy weather, and the impact of dirt particles on the panel.

Author contributions

Shoab Shaikh: Conceptualization, Data curation, Formal analysis, Validation, Visualization, Writing - original draft, Writing - review & editing. Syed Hadi Hussain Shah: Investigation, Resources, Software,



Table 9

Summary of comparison of three algorithms.

| Algorithm | Speed   | Accuracy                       | No initial Guesses | Input Variables               | Oscillation @ MPP | Stability |
|-----------|---------|--------------------------------|--------------------|-------------------------------|-------------------|-----------|
| P&C       | Fastest | Accurate                       | 1                  | Solar irradiance, Temperature | No                | Yes       |
| BSM       | Medium  | It is accurate but may deviate | 2                  | Solar irradiance, Temperature | No                | Yes       |
| P&O       | Slowest | Accurate                       | 0                  | Voltage, Current of PV panel  | Yes               | Yes       |

Supervision, Validation, Visualization, Writing - original draft, Writing - review & editing. Lyu Guanghua: Data curation, Formal analysis, Funding acquisition, Investigation. Arsalan Muhammad Soomar: Conceptualization, Formal analysis, Supervision, Validation, Writing - original draft, Writing - review & editing. Muhammad Mohsin Aman: Conceptualization, Data curation, Formal analysis, Supervision, Validation, Visualization, Writing - original draft. Farah Andleeb Siddiqui: Conceptualization, Data curation, Formal analysis, Investigation, Methodology, Project administration, Resources, Software, Validation, Writing - original draft. Aqsa Ali: Methodology, Project administration, Resources, Software, Validation, Visualization, Writing - original draft

### Declaration of competing interest

The authors declare that they have no known competing financial interests or personal relationships that could have appeared to influence the work reported in this paper.

### Data availability

Data will be made available on request.

### Acknowledgments

All authors have helped complete this paper, and we would like to express our gratitude to Power China Huadong Engineering Co., Ltd., Hangzhou, China, for their assistance in data collection.

### References

- [1] A. Ben Zid, A. Lamari, F. Bacha, Seven-level grid-connected packed U-cells inverter using photovoltaic generators system, in: Proceedings of the Institution of Mechanical Engineers, Part I: Journal of Systems and Control Engineering, vol. 237, 2023, pp. 684–703, <https://doi.org/10.1177/0959651820987955>, 4.
- [2] P.K. Pathak, A.K. Yadav, S. Padmanaban, P.A. Alvi, Design of robust multi-rating battery charger for charging station of electric vehicles via solar PV system, *Electr. Power Compon. Syst.* 50 (14–15) (2022) 751–761, <https://doi.org/10.1080/15325008.2022.2139870>.
- [3] P.K. Pathak, A.K. Yadav, Design of battery charging circuit through intelligent MPPT using SPV system, *Sol. Energy* 178 (2019) 79–89, <https://doi.org/10.1016/j.solener.2018.12.018>.
- [4] L. Abualigah, R.A. Zitar, K.H. Almotairi, A.M. Hussein, M. Abd Elaziz, M.R. Nikoo, A.H. Gandomi, Wind, solar, and photovoltaic renewable energy systems with and without energy storage optimization: a survey of advanced machine learning and deep learning techniques, *Energies* 15 (2) (2022) 578.
- [5] L. Chen, W. Han, Y. Shi, J. Zhang, S. Cao, A photovoltaic parameter identification method based on Pontogammarus maoticus swarm optimization, *Front. Energy Res.* 11 (2023) 1204006, <https://doi.org/10.3389/FENRG.2023.1204006>.
- [6] P.K. Pathak, A.K. Yadav, P.A. Alvi, A state-of-the-art review on shading mitigation techniques in solar photovoltaics via meta-heuristic approach, *Neural Comput. Appl.* 34 (1) (2022) 171–209, <https://doi.org/10.1007/s00521-021-06586-3>.
- [7] J.A. Gow, C.D. Manning, Development of a photovoltaic array model for use in power-electronics simulation studies, *IEEE Proc. Elec. Power Appl.* 146 (2) (1999) 193–200.
- [8] K. Nishioka, N. Sakitani, Y. Uraoka, T. Fuyuki, Analysis of multicrystalline silicon solar cells by modified 3-diode equivalent circuit model taking leakage current through periphery into consideration, in: *Solar Energy Materials and Solar Cell*, vol. 91, Elsevier, 2007, pp. 1222–1227.
- [9] C. Carrero, J.A. Guerra, S. Arnalte, A single procedure for helping PV designers to select silicon PV modules and evaluate the loss resistances, *Renew. Energy* 32 (2007) 2579–2589.
- [10] M.G. Villalva, J.R. Gazoli, E.R. Filho, Comprehensive approach to modeling and simulation of photovoltaic arrays, *IEEE Trans. Power Electron.* 24 (2009) 1198–1208.
- [11] I. Haider, A. Nader, Variations of PV Module Parameters with Irradiance and Temperature, Elsevier (*Energy Procedia*), 5–7 July 2017, pp. 276–285.
- [12] R.B. Bollipo, S. Mikkili, P.K. Bonthagorla, Critical review on pmppt techniques: classical, intelligent and optimisation, *IET Renew. Power Gener.* 14 (9) (2020) 1433–1452.
- [13] A.A. Abdulrazzaq, A. Hussein Ali, Efficiency performances of two MPPT algorithms for PV system with different solar panels irradiancess, *Int. J. Power Electron. Drive Syst.* 9 (4) (2018) 1755, <https://doi.org/10.11591/ijpeds.v9.i4.pp1755-1764>.
- [14] H.A.B. Siddique, P. Xu, R.W.D. Doncker, Parameter extraction algorithm for one-diode model of PV panels based on datasheet values, in: Presented at the International Conference on Clean Electrical Power (ICCEP), Alghero, Italy, 2003.
- [15] A. Aamir, A. Aamir, J. Selvaraj, N.A. Rahim, Study the MPPT Algorithms: Focusing on Numerical Methods Technique, Elsevier (*Renewable and Sustainable Energy Reviews*), 2016.
- [16] S. Chun, A. Kwasinski, Analysis of classical root-finding methods applied to digital maximum power point tracking for sustainable photovoltaic energy generation, *IEEE Trans. Power Electron.* 26 (2011) 3730–3743.
- [17] B. Bendib, H. Belmili, F. Krim, A Survey of the Most Used MPPT Methods: Conventional and Advanced Algorithms Applied for Photovoltaic Systems, Elsevier (*Renewable and Sustainable Energy Reviews*), 2015, pp. 637–648.
- [18] Y.T.D. Nesi'c, W.H. Moase, C. Manzie, A unifying approach to extremum seeking: adaptive schemes based on estimation of derivatives, in: 49th IEEE Conference on Decision and Control, Hilton Atlanta Hotel, Atlanta, GA, USA, 2010.
- [19] A. Ghaffari, M. Krstic, D. Nesi'c, Multivariable Newton-based Extremum Seeking, vol. 48, Elsevier(*Automatica*), 2012.
- [20] S.H. Hosseini, A. Farakhor, S.K. Haghghighian, Novel algorithm of MPPT for PV array based on variable step Newton-raphson method through model predictive control, in: Presented at the 13th International Conference on Control, Automation and Systems, Gwangju, Korea, 2013.
- [21] I. Houssamo, F. Locment, M. Sechilariu, Maximum Power Tracking for Photovoltaic Power System: Development and Experimental Comparison of Two Algorithms, Elsevier (*Renewable Energy*), 2010, pp. 2381–2387.
- [22] S.J. Moura, Y.A. Chang, Lyapunov-based Switched Extremum Seeking for Photovoltaic Power Maximization, vol. 21, Elsevier (*Control Engineering Practice*), 2013, pp. 971–980.
- [23] P. Merhej, Solar Cell Modellization and Power Management in Photovoltaic Generation System, 2009.
- [24] M. Uoya, H. Koizumi, A calculation method of photovoltaic array's operating point for MPPT evaluation based on one-dimensional Newton-raphson method, *IEEE Trans. Ind. Appl.* 51 (2015) 567–575.
- [25] H. Zazo, R. Leyva, E.d. Castillo, MPPT based on Newton-like extremum seeking control, *IEEE International Symposium on Industrial Electronics* (2012) 1040–1045.
- [26] S. Shaikh, S. Shaikh, A.M. Soomar, S.H.H. Shah, Coordination of protective relays in the substation, *Int. J. Power Electron. Drive Syst.* 14 (3) (2023) 1471, <https://doi.org/10.11591/ijpeds.v14.i3.pp1471-1478>.
- [27] S. Chun, A. Kwasinski, Modified Regula Falsi optimization method approach to digital maximum power point tracking for photovoltaic application, in: Twenty-Sixth Annual IEEE Applied Power Electronics Conference and Exposition, APEC), Fort Worth, TX, USA, 2011.
- [28] J. Ma, K.L. Man, T.O. Ting, N. Zhang, S.U. Guan, P.W.H. Wong, et al., Improving power-conversion efficiency via a hybrid MPPT approach for photovoltaic systems, *ELEKTRONIKA IR ELEKTROTEHNIKA* 19 (2013) 57–60.
- [29] J. Ma, K.L. Man, T.O. Ting, N. Zhang, C.-U. Lei, N. Wong, A hybrid MPPT method for photovoltaic systems via estimation and revision method, in: *IEEE International Symposium on Circuits and Systems*, 2013. Beijing, China.
- [30] P. Wang, H. Zhu, W. Shen, F.H. Choo, P.C. Loh, K.K. Tan, A novel approach of maximizing energy harvesting in photovoltaic systems based on bisection search theorem, in: Twenty-Fifth Annual IEEE Applied Power Electronics Conference and Exposition (APEC), 2010. Palm Springs, CA, USA.
- [31] J. Ma, K.L. Man, T.O. Ting, N. Zhang, C.-U. Lei, N. Wong, Low-cost global MPPT scheme for Photovoltaic systems under partially shaded conditions, in: Presented at the IEEE International Symposium on Circuits and Systems, 2013. Beijing, China.
- [32] L. Chen, A. Amirahmadi, Q. Zhan, N. Kutkut, I. Batarseh, Design and implementation of three-phase two-stage grid-connected module integrated converter, *IEEE Trans. Power Electron.* 29 (2014) 3881–3892.
- [33] Q. Zhang, C. Hu, L. Chen, A. Amirah, N. Kutkut, Z.J. Shen, et al., A center point iteration MPPT method with application on the frequency-modulated LLC microinverter, *IEEE Trans. Power Electron.* 29 (2013) 1262–1274.
- [34] M. Sheikholeslami, Numerical analysis of solar energy storage within a double pipe utilizing nanoparticles for expedition of melting, *Sol. Energy Mater. Sol. Cell.* 245 (2022) 111856.
- [35] L.G. Hua, Q.A. Memon, M.F. Shaikh, S.A. Shaikh, R.A. Rahimoon, S.H.H. Shah, A. Qadir, Comparative analysis of power output, fill factor, and efficiency at fixed and variable tilt angles for polycrystalline and monocrystalline photovoltaic panels—the case of sukkr IBA university, *Energies* 15 (11) (2022), <https://doi.org/10.3390/EN15113917>.

- [36] M. Dowell, P. Jarratt, A modified regula falsi method for computing the root of an equation, *BIT Numerical Mathematics* 11 (1971) 168–174.
- [37] A.M. Soomar, A. Hakeem, M. Messaoudi, P. Musznicki, A. Iqbal, S. Czapp, Solar photovoltaic energy optimization and challenges, *Front. Energy Res.* 10 (2022), <https://doi.org/10.3389/fenrg.2022.879985>.
- [38] A.M. Soomar, L. Guanghua, S. Shaikh, S.H.H. Shah, P. Musznicki, Scrutiny of power grids by penetrating PV energy in wind farms: a case study of the wind corridor of Jhampir, Pakistan, *Front. Energy Res.* 11 (2023), <https://doi.org/10.3389/fenrg.2023.1164892>.